Deep Learning-Based Image Classification of 18650 Lithium-Ion Battery Structural Health Using X-ray Micro-Computed Tomography

Justin An , Aigbe Emmanuel Awenlimobor , Jiajun Xu * , Miaomiao Ma

Posted Date: 15 May 2026

doi: 10.20944/preprints202605.1010.v1

Keywords: convolutional neural network; deep learning; lithium-ion batteries; structural health; transfer learning

 doi:10.20944/preprints202605.1010.v1

Article

Deep Learning-Based Image Classification of 18650 Lithium-Ion Battery Structural Health Using X-ray Micro-Computed Tomography

Justin An [1], Aigbe Awenlimobor [1], Jiajun Xu [1,*] and Miaomiao Ma [2]

[1] School of Engineering and Applied Sciences, University of the District of Columbia, Washington, DC 20008, USA

[2] Naval Surface Warfare Center Carderock Division, West Bethesda, MD 20817, USA

* Correspondence: jiajun.xu@udc.edu

Abstract

Lithium-ion batteries (LIBs) are ubiquitous in modern technology, powering consumer electronics, electric vehicles, and energy-storage systems. As these systems age, internal structural degradation can lead to reduced performance, diminished lifetime, and increased safety risks, including thermal instability. Because many forms of degradation occur internally and are not detectable through external measurements, accurate assessment of structural health can be observed by non-destructive imaging and robust analysis techniques. In this study, a transfer learning-based deep learning framework for classifying the structural health conditions of 18650-format LIB cells using X-ray micro-computed tomography (μCT) imaging is proposed. This approach includes preprocessing that extracts radial CT slices and core-region cropping to capture localized 3D structure. The dataset is balanced and augmented with transformations and rotations, and a pretrained InceptionResNet-V2 model is fine-tuned to distinguish between various cell conditions. Modified classification layers with dropout and class weighting improve robustness. Initial results demonstrate that the model can identify internal structural differences with promising accuracy, supporting the development of automated μCT-based battery health assessment and safety diagnostics.

Keywords: convolutional neural network; deep learning; lithium-ion batteries; structural health; transfer learning

1. Introduction

Lithium-ion batteries are used extensively throughout the world, as it serves as one of the most dominant energy storage technologies in modern society [1]. It is used in most modern-day electronics, electric vehicles (EVs), and grid renewable energy storage [2]. Their widespread use is due to their high energy density, long cycle life, and relatively low self-discharge rate [3]. Despite these advantages, lithium-ion batteries inevitably degrade over time because of mechanical, chemical, and thermal usage. The internal changes that accompany this degradation include electrode delamination, separator shrinkage, jelly roll deformation, and the formation of microcracks [4]. These changes reduce the performance of the cells and in some cases can create safety hazards such as internal short circuits and thermal runaway.

Traditional methods for assessing the health of a lithium-ion battery often rely on external electrochemical measurements such as capacity retention, impedance spectroscopy, and voltage analysis [5]. While these methods allow for the assessment of the overall performance of a cell, they provide limited information about internal structural changes [6], [7]. Due to this reason, there is increasing interest in the use of imaging techniques to directly observe and quantify these internal features [8], [9]. X-ray micro computed tomography (μCT) is one such technique. It provides a nondestructive and high-resolution three-dimensional (3D) view of the internal architecture of a

 doi:10.20944/preprints202605.1010.v1

battery cell, enabling researchers to examine key components including electrodes, separators, current collectors, and the jelly roll arrangement [10], [11]. This allows for the detection of defects and the mapping of structural changes throughout the battery's life cycle without the need for physical disassembly [12].

Although μCT produces highly detailed images, interpreting these datasets manually is both time-consuming and subject to human bias [13]. The large volume of image slices generated for a single scan presents a challenge for analysis, particularly when the objective is to detect subtle changes across many samples. Advances in artificial intelligence, particularly in the area of deep learning, have created opportunities to automate this process. Convolutional neural networks (CNNs) have been successfully used in areas such as medical imaging, materials science, and industrial quality control to classify complex image data with high accuracy [14], [15]. In cases where available data is limited, transfer learning provides an effective approach to resolve this issue. In this technique, a CNN that has been trained on a large and diverse image dataset is adapted to a new domain by fine-tuning its parameters. This reduces the need for an extensive battery-specific training set while retaining the feature extraction capabilities of the original model.

The work presented in this study applies transfer learning to the classification of internal structural conditions in 18,650 format lithium-ion battery cells using images obtained from X-ray μCT tomography. The dataset used includes cells that are pristine, cycle-aged, thermally cycled and calendar-aged (high-temperature storage). To improve the feature extraction aspect, domain-specific preprocessing is used, where we incorporate centroid-based core cropping and three-slice stacking to capture localized three-dimensional structural information. These processed images are then used to fine-tune a deep convolutional neural network based on the InceptionResNetV2 architecture. The objective is to develop a classification framework that is accurate, efficient, and scalable. The proposed approach aims to support predictive maintenance, improve quality assurance, and enhance safety monitoring for lithium-ion battery systems in practical applications.

2. Materials and Methods

The experimental data was collected using the Scanco X-ray 100 cabinet μCT scanner. Figure 1 illustrates the scanner used, the holder used and an 18,650 LIB cell. In Figure 1(a), the full view of the cabinet can be seen. Figure 1(b) shows the rotary stand for which we can place sample holders containing samples for measurement. Figure 1(c) is schematic of the scanning process, in which X-rays emitted from the source penetrate the lithium-ion battery sample.

(**a**) (**b**) (**c**)

Figure 1. Battery μCT scanning equipment. (a) Scanco μCT 100 cabinet scanner (b) closer view of the cabinet showing the μCT sample holders (c) 35 mm holder shown alongside an 18,650 LIB cell.

The detector captures the transmitted X-rays after they pass through the sample and converts them into digital signals, which are then used for image reconstruction. Figure 2 illustrates the schematic of the micro-CT scanning process. In this setup, X-rays are emitted from the source and

 doi:10.20944/preprints202605.1010.v1

directed toward the battery sample mounted on a rotating platform. As the X-rays penetrate the sample, variations in material density and internal structure attenuate the beam differently. The transmitted X-rays are then recorded by the detector, producing a series of projection images at multiple angles. These projections are subsequently reconstructed to generate high-resolution cross-sectional images that reveal the internal morphology of the battery.

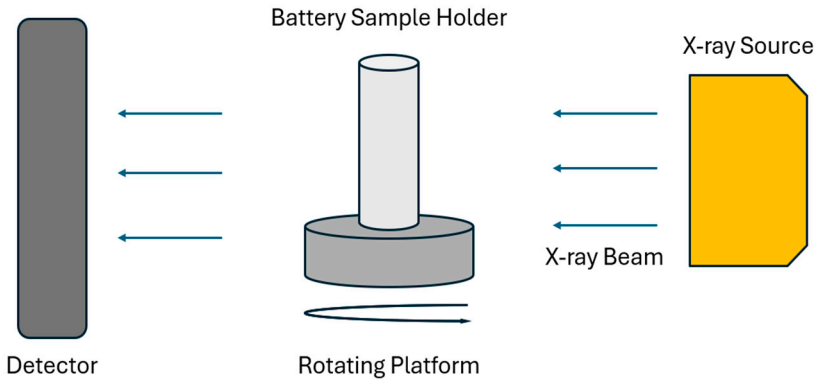

Figure 2. Diagram of scanning process. X-ray is emitted from the source, then penetrates the sample to obtain the internal images on the detector.

The specifications and capabilities of the Scanco X-ray 100 cabinet μCT scanner are shown in Table 1. The cabinet scanner allows for nondestructive 3D imaging of small-to-medium-sized samples, enabling detailed internal structure analysis at micrometer-scale resolution. The enclosed cabinet design provides both radiation shielding for operator safety and mechanical stability for consistent scanning conditions.

Table 1. Specifications of the SCANCO μCT Cabinet Scanner.

Specifications	Details
Imaging Resolution	Down to 6 μm voxel size
X-Ray Source	Micro-focus X-ray tube
Detector	2D Flat Panel Detector
Scan Modes	High-resolution 3D imaging (<4μm 10% MTF), tomography, and dynamic scanning
Field of View	Up to 30 mm (depending on detector and resolution)
Sample Size	Max sample size of 50 mm in diameter
Scanning Time	Varies with resolution and sample size (typically minutes to hours)
Reconstruction Time	~10-60 minutes, depending on scan parameters
3D Visualization	Provided advanced segmentation and analysis tools

The scans were conducted at an operating voltage of 90 kV and a current of 200 μA, corresponding to a total power output of 18 W. These parameters were chosen to provide sufficient X-ray penetration through the dense electrode and current collector materials of the 18,650 lithium-ion cells while maintaining high image contrast. An air filter was used to reduce beam hardening effects, and the system's default calibration settings were applied to ensure measurement consistency across all samples. The high-resolution mode was selected to capture detailed structural features, such as electrode layer spacing and micro-scale defects, which are essential for accurate structural health assessment. Each cell was mounted in a 35 mm sample holder designed for cylindrical samples. Reconstruction times ranged from 30 minutes to 2 hours depending on the acquisition parameters, and the system can accommodate samples with diameters up to 50 mm. The operating parameters used for high resolution imaging of the lithium-ion battery cells are provided in Table 2.

 doi:10.20944/preprints202605.1010.v1

Table 2. Data collection X-Ray imaging scanning parameters used.

Battery Test Parameters	Details
X-Ray Voltage	90 kV
Working Current	200 μA
Power Output	18 W
Filter	Air
Calibration	Default
Resolution	High
Sample Holder Size	35 mm

2.1. InceptionResNetV2 Architecture

In this study, InceptionResNet-V2, a convolutional neural network pretrained on the ImageNet dataset, is used as the foundation for the transfer-learning framework. This architecture combines the representational strength of deep residual connections with the multi-scale feature extraction capabilities of Inception modules, making it suited for identifying the subtle morphological changes present in X-ray micro-CT images of lithium-ion batteries suited for identifying the subtle morphological changes present in X-ray micro-CT images of lithium-ion batteries.

InceptionResNetV2 combines the strengths of Inception modules and residual connections within a single architecture. This hybrid design enables the network to efficiently capture features at multiple spatial scales while maintaining stable training behavior. Residual connections allow information to flow through deep networks without degradation, reducing training difficulty and improving convergence speed. Additionally, the use of parallel convolutional paths with different kernel sizes within Inception blocks allows the model to learn both fine-scale and coarse-scale structural patterns simultaneously.

The architecture is composed of multiple stacked blocks that integrate convolutional layers, feature merging, nonlinear activation functions, and residual pathways. This design has demonstrated strong performance in complex image analysis tasks, particularly in domains where subtle structural differences must be identified. For this reason, InceptionResNetV2 was selected as the pre-trained backbone for this study, providing a robust and transferable feature extraction foundation for classifying structural health conditions in micro-CT images of lithium-ion batteries.

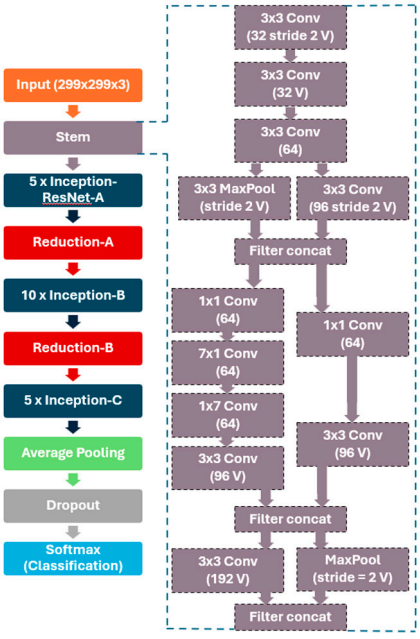

Figure 3. Schematic of Inception-Resnet-v2 network.

 doi:10.20944/preprints202605.1010.v1

2.2. Dataset Preparation

The dataset used for training consists of four classes of images of CT scanned images. The training and validation data is shown in Table 3. The data is divided into training and validation datasets of 80% and 20%, respectively.

Table 3. Dataset details for the proposed algorithm.

Dataset	Number of total images	Training data (80%)	Validation data (20%)
Pristine	340	272	68
Cycle-aged	340	272	68
Calendar-aged	340	272	68
Thermal-Cycle	340	272	68

In total, 340 images were used for each class. For the training set, 272 images were used, and 68 images were used for validation. 340 images were used for each class to avoid overfitting. The following Figure 4 shows the digital reconstruction of the CT scans done for the pristine and the cycle-aged cell, and a zoom-enhanced image of the core winding region.

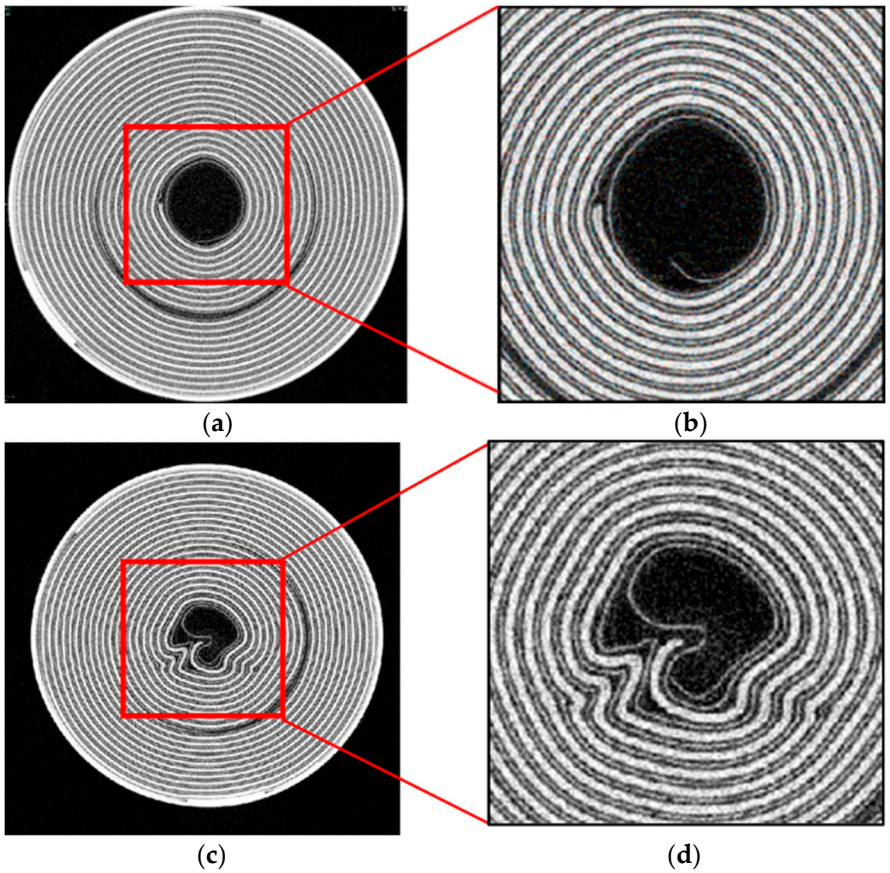

Figure 4. (a) Axial scan of pristine cell (b) winding region of pristine cell (c) axial scan of thermally-cycled cell (d) winding region of thermally-cycled cell.

Figures 4(a) and 4(c) show full radial cross-sectional CT scans of a pristine cell and a thermally-cycled cell, respectively. Figures 4(b) and 4(d) present magnified views of the highlighted regions, allowing for comparison of the internal electrode structure. The pristine cell exhibits a uniform and concentric winding pattern, while the thermally-cycled cell shows noticeable distortion and irregularities in the winding geometry. Figure 5 presents representative cropped μCT images

 doi:10.20944/preprints202605.1010.v1

highlighting the internal structural differences among the four lithium-ion battery conditions considered in this study.

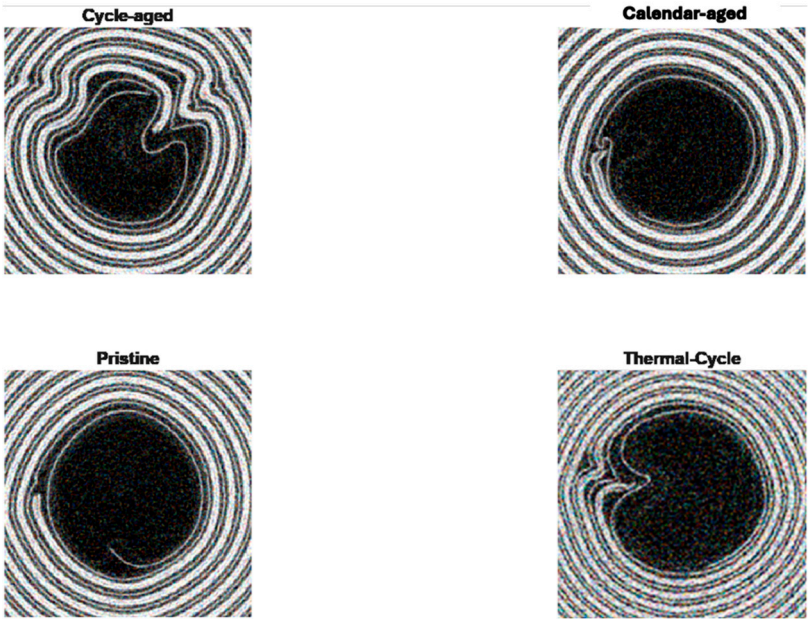

Figure 5. Representative cropped μCT images of lithium-ion battery cells under different structural conditions.

Each battery condition exhibits distinct structural characteristics within the electrode winding region. The cycle-aged cell exhibits the most severe structural disruption, with significant warping and non-uniform spacing throughout the electrode layers. The calendar-aged cell shows slight irregularities and localized deviations near the core, suggesting gradual degradation over time. The pristine cell displays a highly uniform and concentric spiral structure, indicating minimal deformation and consistent electrode spacing. More pronounced deformation is observed in the thermal-cycle condition, as distortion of the winding structure becomes more evident due to repeated thermal stress. These visual differences demonstrate how various aging mechanisms impact the internal morphology of lithium-ion batteries and provide the basis for feature extraction in the proposed deep learning model.

2.3. Preprocessing

The X-ray micro computed tomography image dataset was preprocessed in MATLAB to ensure consistency in spatial resolution, structural focus, and compatibility with the deep learning framework prior to model training. All CT images were organized into class-labeled subfolders corresponding to the four lithium-ion battery structural conditions investigated in this study.

To adapt the network for CT-based structural classification, several domain-specific modifications were introduced. First, radial slices from the CT images were obtained from the scanner. Then, the battery's central winding region is extracted using an automated center-crop operation. To provide 3-dimensional, three adjacent slices are stacked into an RGB-like representation, allowing the pretrained 2D network to capture inter-slice continuity without requiring a full 3D model. These stacked samples are then normalized, contrast-corrected, augmented with transformations, and the number of images were balanced across all battery conditions to prevent class bias.

Data augmentation was applied to the training dataset using small, controlled geometric transformations. These augmentations include limited rotations, translations, and scaling operations.

 doi:10.20944/preprints202605.1010.v1

Table 4. Data augmentation parameters used.

Augmentation	Values
Rotation	−5° to +5°
Horizontal translation	−10 to +10 pixels
Vertical translation	−10 to +10 pixels
Horizontal scaling	0.95 to 1.05
Vertical scaling	0.95 to 1.05
Image resizing	299 × 299 pixels

2.4. Proposed Algorithm

The proposed convolutional neural network, referred to as NewNet, is built upon the pretrained InceptionResNet-V2 architecture and is designed to classify lithium-ion battery structural conditions from X-ray micro computed tomography (μCT) images. The network processes input images in a sequential, layer-by-layer manner, where progressively deeper layers extract increasingly complex representations of internal battery structure. This hierarchical feature extraction enables the model to distinguish subtle differences among pristine, cycle-aged, calendar-aged, and thermally cycled cells based on their internal deformation patterns.

InceptionResNet-V2 serves as the backbone of the proposed framework, leveraging its deep convolutional layers and residual connections to extract robust and multi-scale visual features. The early layers of the network retain their pretrained weights to capture general low-level patterns such as edges, gradients, and textures, while the deeper layers are fine-tuned to learn battery-specific structural signatures. These signatures include variations in core symmetry, spiral winding distortion, void formation, and localized density irregularities that arise from aging and thermal abuse. Residual connections within the architecture facilitate efficient gradient flow during training, allowing the network to learn deep representations without degradation in performance.

To adapt the pretrained model for the battery classification task, the original classification head is removed and replaced with a custom task-specific head. This new head consists of multiple dropout layers for regularization, an intermediate fully connected layer that enhances feature abstraction, and a final fully connected layer sized to the number of battery condition classes. A SoftMax activation function converts the network outputs into class probabilities, followed by a class-weighted classification layer that mitigates the influence of residual class imbalance during training.

All input images are resized to 299 × 299 × 3 pixels to match the input requirements of InceptionResNet-V2. Because the original μCT images are grayscale, a three-slice stacking approach is used, where three adjacent axial slices are combined into an RGB-like representation. This strategy allows the two-dimensional network to capture limited three-dimensional structural continuity without the computational cost of full 3D convolutional models. Additionally, a centroid-based cropping technique is used to isolate the central winding region of the battery. This focused cropping ensures that the model concentrates on the most structurally relevant features while reducing background variability. The images are further normalized and contrast-adjusted to ensure consistency across the dataset.

Training is performed using the cross-entropy loss function and the Adam optimizer with an initial learning rate of 0.0001. The network is trained for approximately 12 to 20 epochs, depending on convergence behavior observed during validation. To improve generalization and reduce overfitting, data augmentation techniques including small random rotations, translations, and scaling are applied during training. These augmentations are intentionally constrained to preserve deformation-related features while increasing dataset diversity. GPU acceleration is used throughout training to enable efficient optimization and rapid experimentation with architectural and hyperparameter configurations.

Among several pretrained architectures evaluated, including ResNet, GoogleNet, VGG variants, and AlexNet, InceptionResNet-V2 showed the most promising performance for this application due to its combination of deep feature extraction, residual learning, and computational efficiency. These

 doi:10.20944/preprints202605.1010.v1

characteristics make it particularly well suited for identifying internal structural degradation in lithium-ion batteries using μCT imaging.

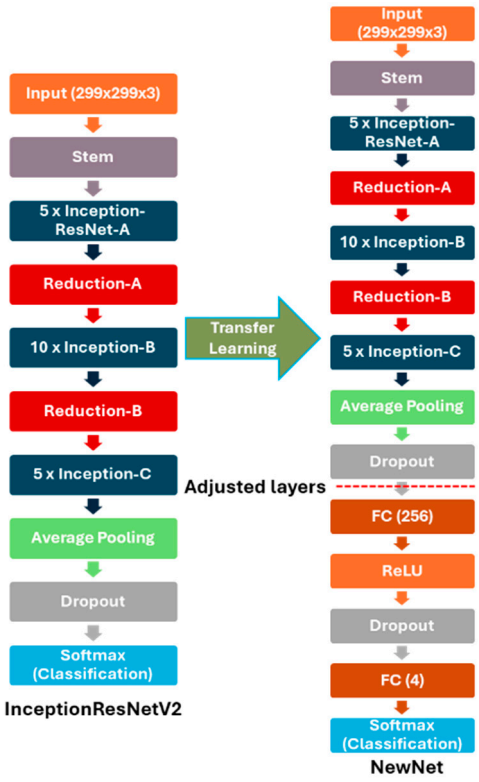

Figure 6. Proposed Transfer learning from InceptionResV2InceptionResNetV2 to NewNet.

3. Results and Discussion

3.1. Model Evaluation

Regarding model evaluation criteria, the standards commonly used in image classification models were applied. These include accuracy, precision, sensitivity, specificity, F1-score. The formulae for these evaluation criteria are detailed below where TP represents true positive, FP represents false positive, FN represents false negative, and TN represents true negative. Together, they provide a comprehensive understanding of the model's predictive behavior, particularly in multi-class classification problems where class imbalance and misclassification costs must be carefully considered.

$$\text{Accuracy} = \frac{T_P+T_N}{T_P+T_N+F_P+F_N} \quad (1)$$

Accuracy represents the proportion of correctly classified samples relative to the total number of test samples. While accuracy provides an overall measure of performance, it does not fully capture how well individual classes are identified, especially when certain classes are more difficult to distinguish.

$$\text{Precision} = \frac{T_P}{T_P+F_P} \quad (2)$$

Precision measures how many of the samples predicted as a given class are correct. A high precision value indicates a low false-positive rate, meaning the model is not frequently mislabeling other battery conditions as that class.

$$\text{Sensitivity} = \frac{T_P}{T_P+F_N} \quad (3)$$

 doi:10.20944/preprints202605.1010.v1

Sensitivity, also referred to as recall, quantifies the model's ability to correctly identify samples belonging to a given class. High sensitivity is particularly important for detecting degradation or abnormal battery conditions, where failing to identify a damaged cell could have safety implications.

$$\text{Specificity} = \frac{T_N}{T_N + F_P} \quad (4)$$

Specificity measures the ability of the model to correctly identify samples that do not belong to a given class, effectively capturing how well false positives are avoided.

$$\text{F1-score} = \frac{2T_P}{2T_P + F_P + F_N} \quad (5)$$

The F1-score combines both precision and sensitivity into a single metric, providing a balanced assessment of classification performance. This metric is particularly useful when evaluating models on datasets where class distributions may vary. Table 5 shows the evaluation metrics per class.

Table 5. Per-class evaluation metrics.

Class	TP	FP	FN	TN	Accuracy	Precision	Sensitivity	Specificity	F1-score
Cycle-aged	44	0	2	102	0.98649	1	0.95652	1	0.97778
Calendar-aged	18	2	0	128	0.98649	0.9	1	0.98462	0.94737
Pristine	46	1	0	101	0.99324	0.97872	1	0.99020	0.98925
Thermal-Cycle	35	2	3	108	0.96622	0.94595	0.92105	0.98182	0.93333

Table 6 shows the overall/macro metrics results for the model evaluation criteria.

Table 6. Model evaluation criteria overall/macro results.

Accuracy (%)	Precision (%)	Sensitivity (%)	Specificity (%)	F1-Score (%)
96.62	95.62	96.94	98.92	96.16

In this study, the model achieved an overall accuracy of 96.62%, indicating that the majority of battery CT images were correctly classified into their respective structural condition categories. The reported macro-averaged precision of 95.62% demonstrates that, on average, the model makes reliable class assignments when it predicts a particular battery condition. The model achieved a macro-averaged sensitivity of 96.94%, indicating strong performance in correctly detecting the true structural condition of batteries across all classes. The high macro-averaged specificity of 98.92% suggests that the model is highly effective at distinguishing between different battery conditions and minimizing incorrect cross-class predictions. The macro-averaged F1-score of 96.16% reflects a strong balance between correctly identifying battery conditions and minimizing misclassification errors. Overall, the reported evaluation metrics indicate that the proposed InceptionResNet-V2-based transfer learning model performs robustly across multiple lithium-ion battery structural conditions. The high accuracy, combined with strong precision, sensitivity, specificity, and F1-score values, demonstrates the model's capability to reliably classify μCT images and effectively capture battery-specific deformation patterns.

3.2. Experimental Results and Analysis

Figure 7 presents the confusion matrix for the proposed NewNet model applied to four lithium-ion battery structural conditions derived from μCT imaging: Cycle-aged, Calendar-aged, Pristine, and Thermally-Cycled. The confusion matrix summarizes the classification performance by comparing the true class labels with the predicted class labels for the test dataset. Diagonal elements represent correctly classified samples, while off-diagonal elements indicate misclassifications between battery conditions.

 doi:10.20944/preprints202605.1010.v1

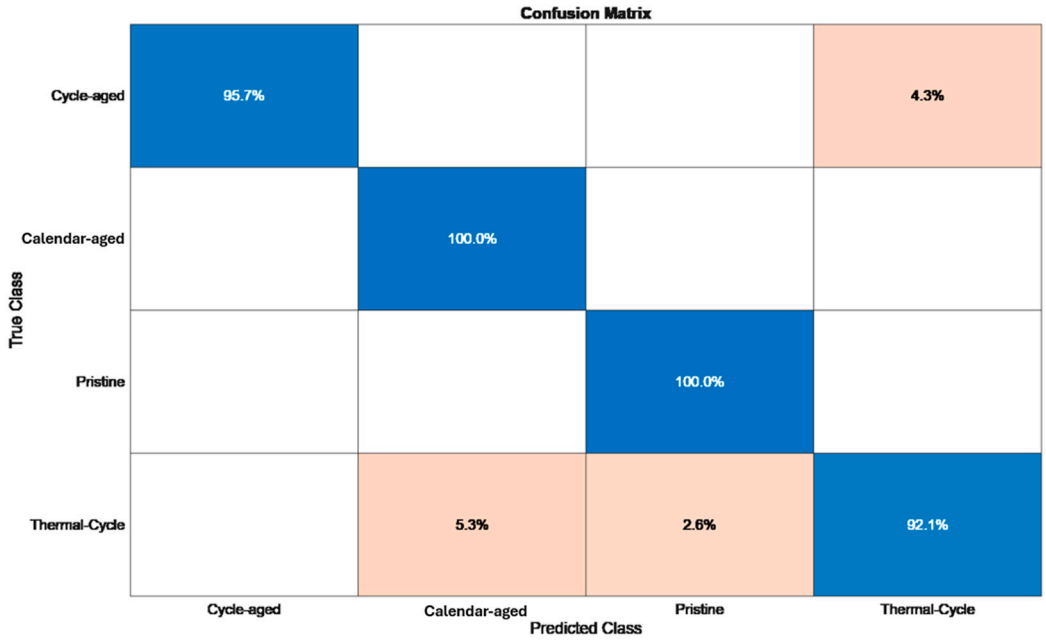

Figure 7. Confusion matrix for NewNet.

The model demonstrates strong classification performance across most classes. Cycle-aged cells are correctly identified with a rate of 95.7%, with a small portion (4.3%) misclassified as Thermally-Cycle, indicating the model identifies some visual similarity between these two degradation mechanisms. Calendar-aged cells achieve perfect classification accuracy, with 100% of samples correctly identified, suggesting that high-temperature-induced structural features are highly distinguishable in the cropped μCT scanned images.

Pristine cells are also classified with high accuracy, achieving a correct classification rate of 100%. Thermal-Cycle cells achieve a correct classification rate of 92.1%, with some confusion between Calendar-aged (5.3%) and Pristine (2.6%) classes. This indicates there are overlapping structural deformation patterns caused by long-term aging processes.

In addition to the class-specific performance shown in the confusion matrix, the overall classification accuracy achieved by the proposed model is 96.62%. This metric reflects the proportion of correctly classified samples across all battery conditions in the test dataset. The high overall accuracy indicates that the combination of core-focused cropping and InceptionResNetV2-based transfer learning enables robust discrimination between pristine, cycle-aged, calendar-aged, and thermally cycled lithium-ion battery cells.

Figure 8 illustrates the NewNet testing predicted results and confidence using the processed X-ray CT scans of 18,650 lithium-ion battery cells for nine randomly chosen images. The reconstructed images can reveal differences in internal electrode structure between pristine, cycle-aged, calendar-aged and thermally cycled cells. The predicted class labels range across multiple structural health states depending on the degree of deformation detected.

 doi:10.20944/preprints202605.1010.v1

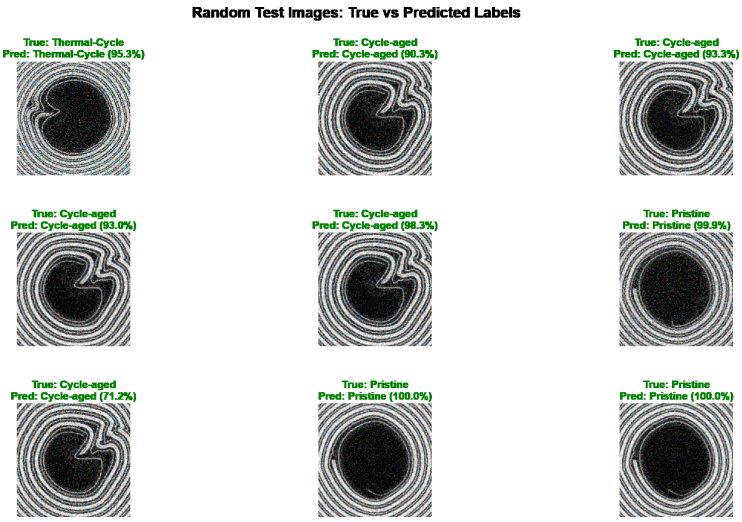

Figure 8. NewNet predicted classification of randomly selected 18,650 LIB images.

Correctly classified samples are predicted with high confidence, often exceeding 90-100%. Pristine classification is noted to have the highest confidence in comparison to the other classes due to its distinct internal structure. On the other hand, thermally cycled cells hover around 90-95% confidence of classification. A majority of the cycle-aged μCT images were classified with a confidence of 90% and above, however, some images hover around 70% confidence. This may be due to confusion between similar internal deformation with another cell. These relatively high confidence values indicate that the model has learned stable and discriminative structural features for these battery conditions. This trend demonstrates that the model's confidence scores provide good results for prediction reliability, with lower confidence often corresponding to ambiguous or transitional structural features.

4. Conclusions

This study demonstrates the feasibility and effectiveness of using deep learning–based transfer learning for non-destructive structural health classification of lithium-ion batteries using X-ray micro-computed tomography data. By combining centroid-based core cropping, three-slice stacking to capture limited three-dimensional context, and fine-tuning of the InceptionResNet-V2 architecture, the proposed framework successfully learns deformation-relevant features directly from internal battery structures. Quantitative evaluation shows strong performance across multiple battery conditions, achieving an overall classification accuracy of 96.62% along with high precision, sensitivity, specificity, and F1-scores.

Detailed analysis of confusion matrices, confidence scores, and visual prediction results reveals that the model is particularly effective at identifying distinct degradation modes such as calendar-aging and thermal cycling, while appropriately expressing uncertainty in cases where structural differences are subtle. Visual inspection further confirms that the model's decisions are grounded in physically meaningful features, including core asymmetry, winding distortion, and density variations within the electrode structure.

Overall, the results highlight the potential of deep learning–assisted CT analysis as a scalable, non-destructive diagnostic tool for lithium-ion battery assessment. The proposed approach offers a pathway toward automated structural health monitoring that can support battery safety evaluation, degradation analysis, and lifecycle management. While the current study focuses on a limited number of degradation categories, future work will aim to expand the dataset, refine degradation labels, and improve sensitivity to early-stage damage, further enhancing the applicability of this framework to real-world battery systems.

 doi:10.20944/preprints202605.1010.v1

Author Contributions: Conceptualization, J.A..; methodology, J.A.; software, J.A.; validation, J.A., M.M., J.X. and A.A.; formal analysis, J.A.; investigation, J.A.; resources, M.M.; data curation, M.M.; writing—original draft preparation, J.A.; writing—review and editing, J.A., A.A., J.X. and M.M.; visualization, J.A.; supervision, J.X. and M.M.; project administration, J.X.; funding acquisition, J.X. All authors have read and agreed to the published version of the manuscript.

Data Availability Statement: The raw data supporting the conclusions of this article will be made available by the authors on request.

Acknowledgments: The authors gratefully acknowledge the technical feedback provided by Dr. Miaomiao Ma of NSWCCD Code 635 throughout the execution of this project, as well as the financial support from the U.S. Naval Sea Systems Command through the NEEC Grant (award #N001782410016) and from NASA under the MUREP Curriculum Award (MCA) (Grant No. 80NSSC23M0198).

Conflicts of Interest: The authors declare no conflicts of interest.

References

1. Peters, J.F.; Baumann, M.; Zimmermann, B.; Braun, J.; Weil, M. The environmental impact of Li-ion batteries and the role of key parameters – A review. Renew. Sustain. Energy Rev. **2017**, 67, 491–506.
2. Ruan, J.; Song, Q.; Yang, W. The application of hybrid energy storage system with electrified continuously variable transmission in battery electric vehicle. *Energy* **2019**, 183, 315–330.
3. Lin, Z.; Li, D.; Zou, Y. Energy efficiency of lithium-ion batteries: Influential factors and long-term degradation. *J. Energy Storage* **2023**, 74, 109386.
4. Kabir, M.M.; Demirocak, D.E. Degradation mechanisms in Li-ion batteries: A state-of-the-art review. *Int. J. Energy Res.* **2017**, 41, 1963–1986.
5. Li, Y.; Maleki, M.; Banitaan, S. State of health estimation of lithium-ion batteries using EIS measurement and transfer learning. *J. Energy Storage* **2023**, 73, 109185.
6. Gervillié-Mouravieff, C.; Bao, W.; Steingart, D.A.; Meng, Y.S. Non-destructive characterization techniques for battery performance and life-cycle assessment. *Nat. Rev. Electr. Eng.* **2024**, 1, 547–558.
7. Evans, D.; Brieske, D.M.; Tebruegge, C.; Kowal, J. Analysis of the impact of manufacturing-induced cell-to-cell variation for high-power applications. *J. Power Sources* **2024**, 614, 235001.
8. Deng, Z.; et al. Recent progress on advanced imaging techniques for lithium-ion batteries. *Adv. Energy Mater.* **2021**, 11, 2000806.
9. Zuo, W.; et al. Nondestructive analysis of commercial batteries. *Chem. Rev.* **2025**, 125, 369–444.
10. X-ray tomography for battery research and development. Available online: https://www.researchgate.net/publication/327268278_X-ray_tomography_for_battery_research_and_development (accessed on 4 December 2025).
11. Huang, C.-J.; et al. X-ray micro-computed tomography for structural analysis of all-solid-state battery at pouch cell level. *ACS Energy Lett.* **2025**, 10, 3459–3470.
12. Evans, D.; Luc, P.-M.; Tebruegge, C.; Kowal, J. Detection of manufacturing defects in lithium-ion batteries—analysis of the potential of computed tomography imaging. *Energies* **2023**, 16, 6958.
13. Khalifa, M.; Albadawy, M. AI in diagnostic imaging: Revolutionising accuracy and efficiency. *Comput. Methods Programs Biomed. Update* **2024**, 5, 100146.
14. Rayed, M.E.; Islam, S.M.S.; Niha, S.I.; Jim, J.R.; Kabir, M.M.; Mridha, M.F. Deep learning for medical image segmentation: State-of-the-art advancements and challenges. *Inform. Med. Unlocked* **2024**, 47, 101504.
15. Zhao, X.; Wang, L.; Zhang, Y.; Han, X.; Deveci, M.; Parmar, M. A review of convolutional neural networks in computer vision. *Artif. Intell. Rev.* **2024**, 57, 99.